WIRELESS COMMUNICATIONS TECHNOLOGIES

Rutgers University, Department of Electrical and Computer Engineering
Course Number: 16:332:559:01 (Advanced Topics in Communication Engineering)
Professor: Narayan Mandayam

Lecture 3 & 4 – Jan. 30th & Feb. 4th, 2002
Summary by Qing Li

Path Loss in Macrocells – Comparison of Hata's Model and Lee's Model

The Path losses using Hata's Model and Lee's Model are plotted in the Figure 1 and Figure 2, where the parameters used are:

Carrier Frequency: 900MHz
BS Height: 70 m
MS Height: 1.5 m

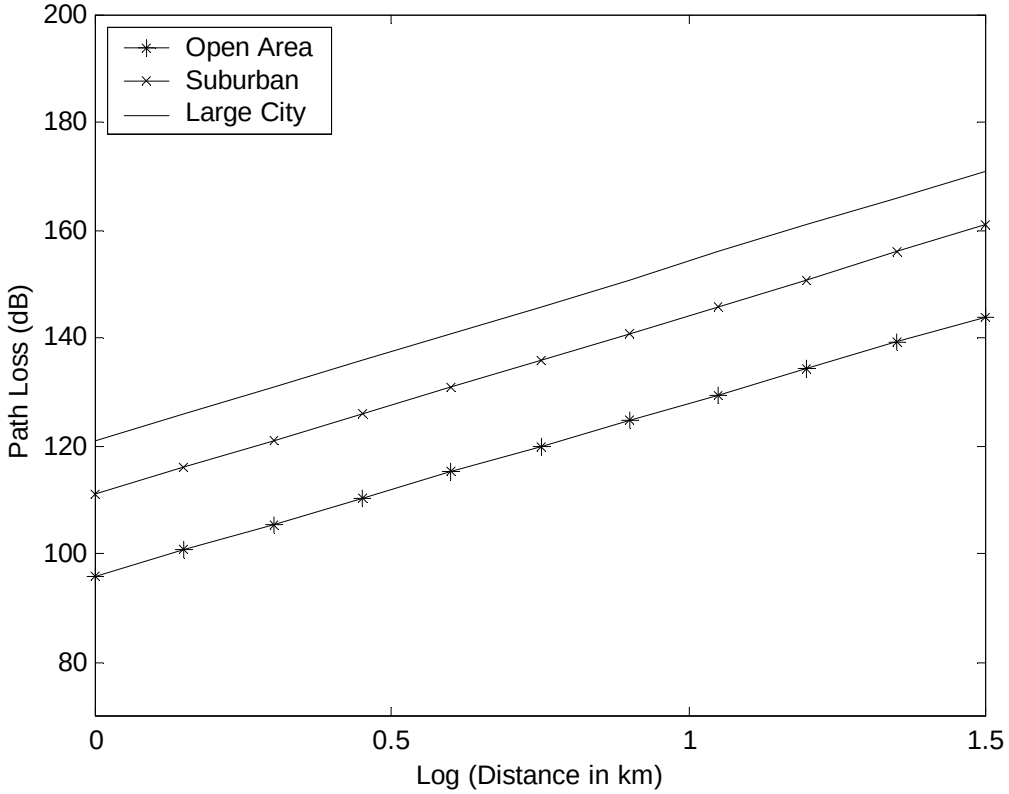

Figure 1: Path Loss obtained by using Hata's Model

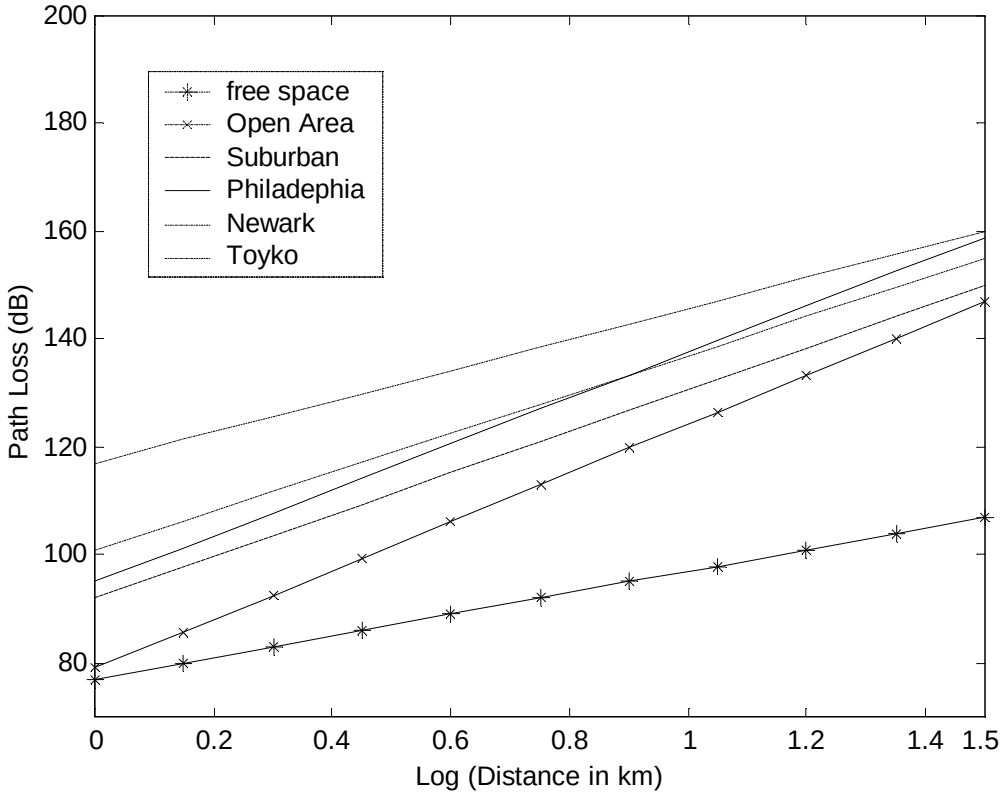

Figure 2: Path Loss obtained by using Lee's Model

Path Loss in Microcells

Most of the future PCS microcellular systems are expected to operate in 1800~2000MHz frequency bands. Some studies have suggested that the pass losses experienced at 1900MHz are approximately 10dB larger than those at 900MHz where all other parameters are kept constant. The COST231 (COST is an intergovernmental framework for European Co-operation in the field of Scientific and Technical Research) study has resulted in two models for urban Microcellular propagation, COST231– Hata Model and COST231–Walfish-Ikegami Model.

COST231 – Hata Model

The COST231– Hata Model extends Hata and Okumura model to 1500~2000MHz where it is known that Hata and Okumura model under estimates the path loss. The parameters used for COST231– Hata Model are:

Carrier Frequency: 1500~2000 MHz
BS Height: 30~200 m
MS Height: 1~10 m

Distance d: 1~20 km

The pass loss can be expressed as

$$Lp = A + B\log_{10}(d) + C$$

Where

$$A = 46.3 + 33.9\log_{10}(f_c) - 13.82\log_{10}(h_b) - a(h_m)$$

$$B = 44.9 - 6.55\log_{10}(h_b)$$

$$C = \begin{cases} 0 & \textit{Medium city and suburban areas with moderate tree density} \\ 3 & \textit{For metropolitan centers} \end{cases}$$

Although both the Okumura and Hata and the COST231 – Hata Model are limited to BS antenna heights greater than 30m, they can be used for lower BS antenna heights provided that the surrounding buildings are well below the BS antenna. They should not be used to predict pass loss in urban canyons. The COST231 – Hata Model is good down to a path length of 1km. It should not be used for smaller ranges, where path loss becomes highly dependent on the local topography.

COST231-Walfish-Ikegami Model

The COST231-Walfish-Ikegami Model is applicable to cases where the BS antennas are either above or below the roof tops. It takes into account parameters such as roof heights, street widths, and road orientation with respect to radio path. The model works best when the BS antennas are much higher than the top of the roof. It is not very accurate when the BS antennas are about the same height as the top of the roof. It is poor when the BS antennas are much lower than the top of the roof because it doesn't consider wave guiding in street canyons and diffraction at street corners.

Path loss in street Microcells ¾ Two-Slope Model

For rangers less than 500m and antenna height less than 20m, some empirical measurements have shown that the received signal strength for LOS propagation along city streets can be accurately described by the two-slope model

$$m_\Omega = 10\log_{10}\left(\frac{A}{d^a(1+d/g)^b}\right) \quad dBm$$

Where

d: Distance in meters

A: Constance

a and b: parameters that reflect path losses ranging from free space to higher. For distance close into the BS, free space propagation will prevail so that *a=2*. At large distances, an inverse-fourth to –eighth power law is experienced so that b ranges from 2 to 6. Note that a and b can be negative value.

g: break point parameter, ranges 150~300m. Breakpoint occurs where the Fresnel zone between the two antennas just touches the ground assuming a flat surface. This distance is

$$g = \frac{1}{l_c}\sqrt{(\Sigma^2 - \Delta^2)^2 - 2(\Sigma^2 + \Delta^2)(\frac{l_c}{2})^2 + (\frac{l_c}{2})^4}$$

Where

$$\Sigma = h_b + h_m$$

$$\Delta = h_b - h_m$$

For high frequencies this distance can be approximated as $g = 4h_b h_m / l_c$. It depends on frequency, with the breakpoint at 1.9GHz being about twice that for 900 MHz.

The model parameters obtained by Harley are listed in the following table,

Base Antenna Height (m)	a	b	Break point g (m)
5	2.30	-0.28	148.6
9	1.48	0.54	151.8
15	0.40	2.10	143.9
19	-0.96	4.72	158.3

Corner Effect

When MS rounds a street corner as shown in Figure 3, LOS changes to NLOS. In this case, average signal strength can drop by 25~30dB over distances as small as 10m for low antenna heights in area with multistory building, and by 25~30dB over distances of 40~50 m for low antenna heights in a region with only one- or two- story building. This is called Corner Effect.

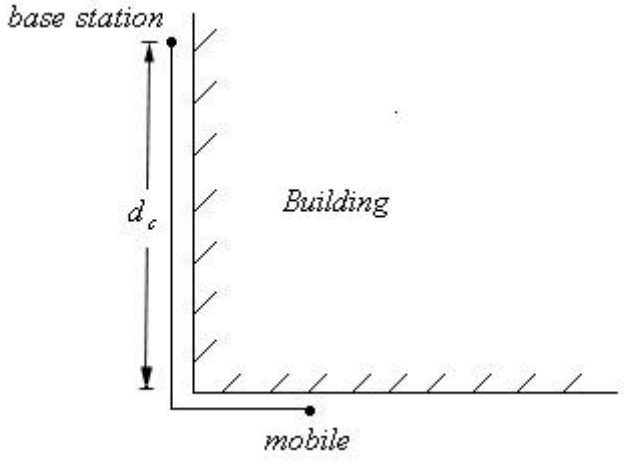

Figure 3: The corner effect in a street microcell environment.

Grimlund and Gudmundson have proposed an empirical street corner path loss model. Their model assumes LOS propagation until the MS reaches a street corner. The NLOS

propagation after rounding a street corner is modeled by assuming LOS propagation from an imaginary transmitter that is located at the street corner having a transmit power equal to the received power at the street corner from the serving BS. The received signal strength (in dBm) is given by

$$m_{\Omega} = \begin{cases} 10\log_{10}\left(\dfrac{A}{d^{a}(1+d/g)^{b}}\right) & d \le d_c \\ 10\log_{10}\left(\dfrac{A}{d_c^{a}(1+d_c/g)^{b}} \cdot \dfrac{1}{(d-d_c)^{a}(1+(d-d_c)/g)^{b}}\right) & d > d_c \end{cases}$$

Where

d_c: the distance between the serving BS and the corner.
d: the distance between BS and MS.

Small-Scale Fading

Small-scale fading is used to describe the rapid fluctuation of the amplitude of a radio signal over a short period of time or travel distance, so that large-scale path loss effects may be ignored. The presence of reflecting objects and scatters in the channel create a constantly changing environment that dissipates the signal energy in amplitude, phase and time. These effects result in multiple versions of the transmitted signals to arrive at the receiver. Each is distorted in amplitude, phase and angle of arrivals. Note here that angle means the direction of the arrivals. The random phase and amplitude of the different multipath components causes fluctuations in signal strength, thereby inducing small-scale fading.

If objects in the radio channel are in motion, they induce a time varying Doppler shift on multipath components. If the surrounding objects move at a greater rate than the mobile, then this effect dominates the small-scale fading. Otherwise, motion of surrounding objects may be ignored, and only the speed of the mobile need be considered.

Now let's consider a two dimension model. A MS moving along the x axis with velocity v, as depicts in Figure 4,

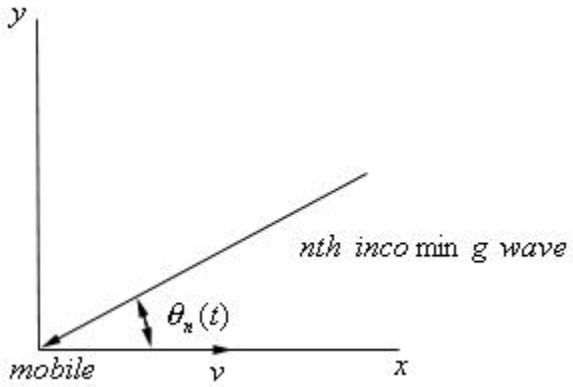

Figure 4: A typical plane wave component incident on a MS receiver

The nth plane wave arrives at the MS antenna with an angle of incidence $q_n(t)$. The MS movement introduced a Doppler frequency shift into the incident plane wave, given by

$$f_{D,n}(t) = f_m \cos q_n(t) = \frac{v}{l_c} \cos q_n(t) \quad Hz,$$

where l_c is the wavelength of the arriving plane wave. Plane waves arriving from the direction of motion will experience a positive Doppler shift, while those arriving opposite from the direction of motion will experience a negative Doppler shift.

Consider the transmission of the band-pass signal

$$s(t) = \mathrm{Re}\{u(t)e^{j2pf_c t}\},$$

where *u(t)* is the complex low-pass signal.

If there are N waves arrive at the receiver, then the received band-pass signal is

$$x(t) = \mathrm{Re}\{r(t)e^{j2pf_c t}\},$$

where the received complex low-pass signal *r(t)* is given by

$$r(t) = \sum_{n=1}^{N} a_n(t)e^{-j2p[(f_c + f_{D,n}(t))t_n(t) - f_{D,n}(t)t]}u(t - t_n(t))$$

where

$a_n(t)$ is the amplitude associated with the nth path,

$t_n(t)$ is the delay associated with the nth path.

The received complex low-pass signal can be rewritten as

$$r(t) = \sum_{n=1}^{N} a_n(t)e^{-j f_n(t)}u(t - t_n(t)),$$

where $f_n(t) = 2p[(f_c + f_{D,n}(t))t_n(t) - f_{D,n}(t)t]$ is the phase associated with the nth path.

So the channel can be modeled by a time-variant filter that having complex low-pass impulse response

$$c(t,t) = \sum_{n=1}^{N} a_n(t)e^{-j f_n(t)}\, d(t - t_n(t))$$

where $c(t,t)$ is the channel response at time t at an input at time $t - t$.

Typically, $f_c + f_{D,n}(t)$ is very large, a small change in the path delay $t_n(t)$ causes a large change in phase $f_n(t)$. At any time t these random phases may result in the constructive or destructive addition of the components. The amplitudes $a_n(t)$ depend on the cross sectional area of the nth scatterer or the length of the nth diffracting surface. However, these quantities do not change significantly over small spatial distances. Therefore, fading is primarily due to time variations in the random phases $f_n(t)$ that are causes by the Doppler shifts $f_{D,n}(t)$.

Received Signal Correlation and Spectrum

It is apparent that the different frequency components in a signal will be affected differently by the small-scale fading channel. However, for narrow-band signals where the signal bandwidth is very small compared to the carrier frequency, it suffices to derive the characteristics of the received complex low-pass signals by considering the

transmission of an unmodulated carrier. For an unmodulated carrier, the received complex low-pass signal is

$$r(t) = \sum_{n=1}^{N} a_n(t) e^{-j f_n(t)} .$$

Since

$$x(t) = \mathrm{Re}\left\{ r(t) e^{j 2 p f_c t} \right\},$$

the received band-pass signal can be expressed in the quadrature form

$$x(t) = r_I(t) \cos 2pf_c t - r_Q(t) \sin 2pf_c t$$

where

$$r_I(t) = \sum_{n=1}^{N} a_n(t) \cos f_n(t)$$

$$r_Q(t) = \sum_{n=1}^{N} a_n(t) \sin f_n(t) .$$

For large N, the central limit theorem can be invoked so that the quadrature components $r_I(t)$ and $r_Q(t)$ can be treated as independent Gaussian random processes. Assuming that these random processes are wide sense stationary (i.e., $f_{D,n}(t) = f_{D,n}$, $a_n(t) = a_n$, and $t_n(t) = t_n$), and assuming that *x(t)* is wide sense stationary, the autocorrelation of *x(t)* is

$$\begin{aligned} f_{xx}(t) &= E[x(t)x(t+t)] \\ &= E[r_I(t) r_I(t+t)] \cos 2pf_c t - E[r_Q(t) r_I(t+t) \sin 2pf_c t \\ &= f_{r_I r_I}(t) \cos 2pf_c t - f_{r_Q r_I} \sin 2pf_c t \end{aligned}$$

Note that

$$f_{r_I r_I}(t) = f_{r_Q r_Q}(t)$$

$$f_{r_I r_Q}(t) = -f_{r_Q r_I}(t) .$$

It is reasonable to assume that the phases $\{f_j(t)\}$ are independent since their associated delays and Doppler shifts are independent. Furthermore, assume $f_n(t)$ uniform distributed over $[-p, p]$. The autocorrelation function for $r_I(t)$ is

$$\begin{aligned} f_{r_I r_I}(t) &= E[r_I(t) r_I(t+t)] \\ &= E\left[\left\{ \sum_{i=1}^{N} a_i \cos f_i(t) \right\} \left\{ \sum_{j=1}^{N} a_j \cos f_j(t+t) \right\} \right] \\ &= \frac{\Omega_p}{2} E_q\left[\cos(2pf_{D,n} t) \right] \end{aligned}$$

where

$$\frac{\Omega_p}{2} = E\left[x^2(t)\right] = E\left[r_I^2(t)\right] = E\left[r_Q^2(t)\right] = \frac{1}{2} \sum_{n=1}^{N} E\left[a_n^2\right]$$

is the total average received power from all multipath components.
Since $f_{D,n} = f_m \cos q_n$, the autocorrelation can be rewritten as

$$f_{r_I r_I}(t) = \frac{\Omega_p}{2} E_q\left[\cos(2pf_m t\cos q)\right]$$

Likewise, the crosscorrelation $f_{r_I r_Q}(t)$ is

$$\begin{aligned} f_{r_I r_Q}(t) &= E[r_I(t) r_Q(t+t)] \\ &= \frac{\Omega_p}{2} E_q\left[\sin(2pf_m t\cos q)\right] \end{aligned}.$$

Two-Dimension Isotropic Scattering

Clarke was the first one suggested that q is uniformly distributed over $[-p, p]$, that is waves arrive with equal probability from all directions. This is called 2-D Isotropic Scattering Model. With the Isotropic Scattering Model, we can rewrite the autocorrelation of $r_I(t)$ as

$$\begin{aligned} f_{r_I r_I}(t) &= \frac{\Omega_p}{2}\frac{1}{2p}\int_{-p}^{p}\cos(2pf_m t\cos q)dq \\ &= \frac{\Omega_p}{2}\frac{1}{p}\int_{0}^{p}\cos(2pf_m t\sin q)dq \\ &= \frac{\Omega_p}{2} J_0(2pf_m t) \end{aligned}$$

Where $J_0(x)$ is the zero-order Bessel function of the first kind. Likewise, we can rewrite the crosscorrelation function as

$$\begin{aligned} f_{r_I r_Q}(t) &= \frac{\Omega_p}{2}\frac{1}{2p}\int_{-p}^{p}\sin(2pf_m t\cos q)dq \\ &= 0 \end{aligned}.$$

The Power spectral density is

$$S_{r_I r_I}(f) = \begin{cases} \dfrac{\Omega_p}{4pf_m}\dfrac{1}{\sqrt{1-(f/f_m)^2}} & |f| \le f_m \\ 0 & otherwise \end{cases}.$$

Since

$$\begin{aligned} r(t) &= r_I(t) + jr_Q(t) \\ f_{r_I r_Q}(t) &= 0 \end{aligned}$$

we have

$$\begin{aligned} f_{rr}(t) &= \frac{1}{2}E[r^*(t) r(t+t)] \\ &= f_{r_I r_I}(t) + j\, f_{r_I\, r_Q}(t) \\ &= f_{r_I r_I}(t) \end{aligned}$$

$$f_{xx}(t) = \mathrm{Re}\left\{f_{rr}(t)e^{j2pf_c t}\right\}$$
$$= \mathrm{Re}\left\{f_{r_I r_I}(t)e^{j2pf_c t}\right\}$$

.

Also note that $f_{r_I r_I}(t) = f_{r_I r_I}{}^*(-t)$ and if *x(t) is real*, $X(w) = X^*(-w)$. It follows the PSD of *x(t)* is

$$S_{xx}(f) = \Im\left\{\frac{f_{r_I r_I}(t)e^{j2pf_c t} + f_{r_I r_I}{}^*(t)e^{-j2pf_c t}}{2}\right\}$$
$$= \Im\left\{\frac{f_{r_I r_I}(t)e^{j2pf_c t} + f_{r_I r_I}(-t)e^{-j2pf_c t}}{2}\right\}.$$
$$= \frac{1}{2}\left[S_{r_I r_I}(f - f_c) + S_{r_I r_I}(-f - f_c)\right]$$

The normalized PSD is plotted against the normalized frequency difference in Figure 5,

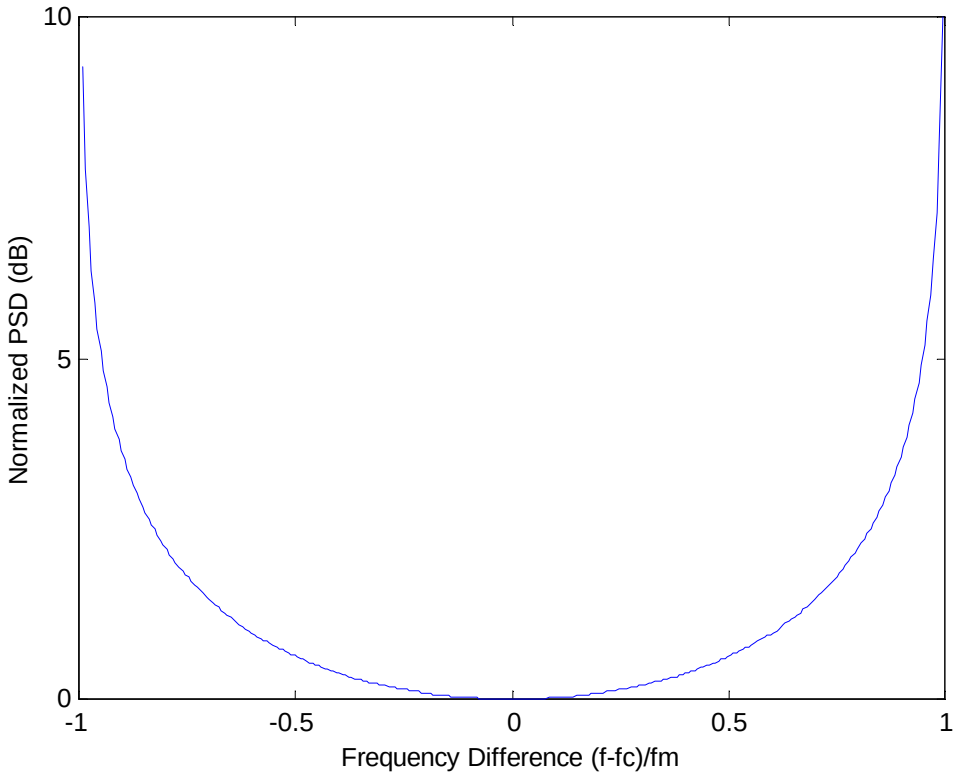

Figure 5: PSD of the received band-pass signal for an isotropic scattering channel.

Received Envelope

Rayleigh Fading

$r(t) = r_I(t) + jr_Q(t)$ is a complex Gaussian process. The question is, for large N, what is the envelope look like? The envelope $z(t) = |r(t)|$ has a Rayleigh distribution at any time t,

$$p_z(x) = \frac{x}{s^2}\exp\left\{-\frac{x^2}{2s^2}\right\} = \frac{x}{\Omega_p/2}\exp\left\{-\frac{x^2}{\Omega_p}\right\} \qquad x \geq 0,$$

where $E[z^2] = \Omega_p = 2s^2$ is the average power. This type of fading is called Rayleigh fading. It applies to any scenario where there is no LOS path between the transmitter and receiver antennas.

The square envelope $Z^2(t) = |r(t)|^2$ is exponentially distributed at any time t,

$$p_{z^2}(x) = \frac{1}{\Omega_p}\exp\left\{-\frac{x}{\Omega_p}\right\} \quad ,$$

where the mean power is Ω_p.

Ricean Fading

When there is a LOS component in addition to NLOS (commonly in microcellular environments), then the complex envelope has a Ricean Distribution at any time t,

$$p_z(x) = \frac{x}{s^2}\exp\left\{-\frac{x^2+s^2}{2s^2}\right\}I_o\left(\frac{xs}{s^2}\right) \qquad x \geq 0,$$

Where

$s^2 = a_0^2\cos^2 q_0 + a_0^2\sin^2 q_0 = a_0^2$ is the non-centrality parameter,

$I_0(\cdot)$ is the modified Bessel function of 0^{th} order,

$K = \frac{s^2}{2s^2}$ characterizes the power in direct path to all the power in non direct path.

When

$K = 0$ the channel exhibits Rayleigh fading,

$K = \infty$ the channel does not exhibit fading.

For a Ricean distributed envelope, the average power is $E[z^2] = \Omega_p = s^2 + 2s^2$ and

$$s^2 = \frac{K\Omega_p}{K+1}, \qquad 2s^2 = \frac{\Omega_p}{K+1},$$

these parameters completely describe the Ricean Fading,

$$p_z(x) = \frac{2x(K+1)}{\Omega_p}\exp\left\{-K - \frac{(K+1)x^2}{\Omega_p}\right\}I_0\left(2x\sqrt{\frac{K(K+1)}{\Omega_p}}\right) \qquad x \geq 0.$$

Nakagami Fading

The Nakagami model is a model purely based on empirical, not on physics. But it is known that it provides a closer match to some experimental data than either the Rayleigh, Ricean or log-normal distributions.

The Nakagami distribution describes the received envelope $z(t) = |r(t)|$ by the distribution

$$p_z(x) = \frac{2m^m x^{2m-1}}{\Gamma(m)\Omega_p^m} \exp\left\{-\frac{mx^2}{\Omega_p}\right\} \qquad m \geq \frac{1}{2},$$

Where $\Omega_p = E[z^2]$. This is called central c^2 distribution with m degrees of freedom. The Nakagami distribution is often used to model multipath-fading for the following reasons. First, the Nakagami destribution can model fading conditions that are either more or less severe than Rayleigh fading. When *m=1*, the Nakagami distribution becomes the Rayleigh distribution. When *m=1/2*, it becomes a one-sided Gaussian distribution, and when $m \to \infty$, it becomes an impulse (no fading). Second, the Ricean distribution can be approximated by using the following relationship,

$$K = \frac{\sqrt{m^2 - m}}{m - \sqrt{m^2 - m}} \qquad m > 1$$

$$m = \frac{(K+1)^2}{2K+1}.$$

Since the Ricean distribution contains a Bessel function while the Nakagami distribution does not, the Nakagami distribution often leads to closed form analytical expressions and insights that are otherwise unattainable.

Frequency-Selective Fading Channel

Small-scale fading considered till now assumes that all frequencies in the transmitted signal are affected similarity by the channel, it is called Frequency Non-Selective or Narrow Band Fading. If the range in the propagation path delays is large compared to the inverse signal bandwidth, then the frequency components in the transmitted signal will experience different phase shifts along different paths. Under this condition the channel introduces amplitude and phase distortion into the message waveform. Such a channel is said to exhibit frequency-selective fading.

Right now we just consider Wide Sense Stationary Uncorrelated Scattering (WSSUS) channels. These channel display uncorrelated scattering in both time-delay and Doppler shift. Fortunately, many radio channels can be accurately modeled as WSSUS channel (Recall, the channel impulse response is $c(t,t)$).

Definition

1. Power Delay Profile (Multipath Intensity Profile) is defined as,

$$f_c(t) = \frac{1}{2} E\left[c(t,t)c^*(t,t)\right].$$

It gives out the average power at the channel output as a function of time delay t. A typical power delay profile is shown in Figure 6,

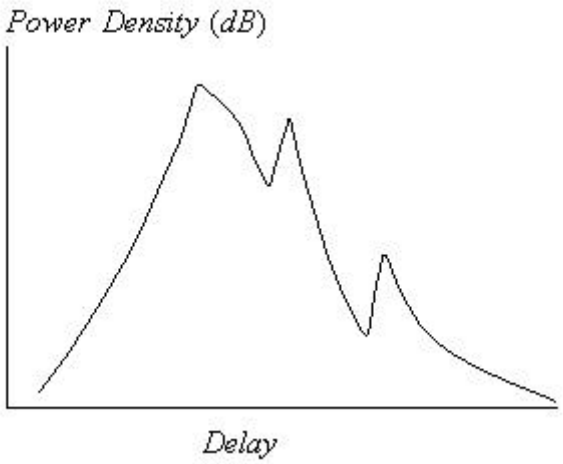

Figure 6: A typical Power Delay Profile

2. Average Delay, defined as,

$$m_t = \frac{\int_0^\infty t\, f_c(t)dt}{\int_0^\infty f_c(t)dt}.$$

3. RMS Delay Spread, defined as

$$s_t = \sqrt{\frac{\int_0^\infty (t - m_t)^2\, f_c(t)dt}{\int_0^\infty f_c(t)dt}}.$$

Where for indoors, the order of RMS delay spread is nanoseconds, it is microseconds for outdoors.

References

[1] G. Stuber, *Principles of Mobile Communication*, Kluwer Academic Publishers, Boston, 1996.

[2] T. Rappaport, *Wireless Communications: Principles and Practice*, Prentice-Hall, NJ, 1996.

[3] P. Harley, "Short Distance Attenuation Measurements at 900MHz and 1.8GHz Using Low Antenna Heights for Microcells", *IEEE Journal Selected. Areas of Communication*, Vol. 7, pp. 5-11, Jan. 1989.

[4] O. Grimlund and B. Gudmundson, "Handoff Strategies in Microcellular Systems", *IEEE Vehicular Technology Conference*, Saint Louis, MO, pp.505-510, May 1991.